Turk J Phys
26 (2002) , 109 – 120.

Relations for Different Resonators of Nd:Glass and Nd:YAG Lasers

Erol TAŞAL, M. Selami KILIÇKAYA
Department of Physics, Osmangazi University, Eskisehir-TURKEY

Received 03.07.2000

Abstract

Simple relations in terms of effective g parameters are given for linear resonators that contain laser rods with curved endfaces and for symmetrical and asymmetric ring resonators of Nd:Glass and Nd:YAG lasers. The equivalence relationships of thick and thin lenses have been applied.

Key Words: Lasers, Resonators, Nd:Glass and Nd:YAG Lasers.

1. Introduction

Solid-state lasers, especially Nd:Glass and Nd:YAG systems, are important high-power light sources for material-processing applications [1]. Many applications of lasers in material processing require a high average or CW output power with high beam quality. Mainly, two laser systems have come to be used in this field: the CO_2 gas laser and the Nd:YAG, ND:Glass solid-state lasers. The solid state lasers have several advantages compared to the CO_2 lasers. Many Studies have been devoted to the optical resanators for these lasers [2]. By using rod resonators, symetrical and asymetric ring resonators, the output power of solid-state lasers can be increased without reducing the beam quality. If a suitable arrangement of rods and mirrors is used, the output power increases proportianally to the number of rods.

The laser-rod heating caused by excitation from the lamps, which induces lens effects that change the resonator properties, is an interesting problem in the design of optimized laser resonators [3]. This problem seems to be even greater with the new generation of solid laser materials [4]. The rod is usually approximated by a thick lens of variable focal length, and the stability regions are described in terms of equivalent g parameters [5, 6, 7]. The laser performance can be summarized as follows: Output energy and peak power in Q–switched operation are comparable to those obtainable with a Nd:YAG rod of comparable dimensions [8]. Output pulse energies of several hundred joules at repetition rates exceeding one per second would be expected, however, using a disc laser where the active medium consists of a stack of glass disk immersed in a liquid coolant. The relevant properties of the resonators, such as the beam size between mirrors, beam–waist location, and stability under pump–induced fluctuations of the focal length, have been analyzed [9, 10, 11]. Compensation for the thermal lens can be achieved with rods that have curved endfaces. Stability analysis has been performed numerically for these resonators. Symmetrical ring resonators have also been analyzed numerically. Rather intricate relations have been used for asymmetric ring resonators.

In this study, simple relations are presented for the resonators of Nd:Glass and Nd:YAG lasers that contain laser rods with curved endfaces. Symmetrical and asymmetric ring resonators are also considered. The stability regions for these resonators are described simply in terms of effective g parameters.

2. Theory

2.1. Equivalence Relations of Thick and Thin Lenses

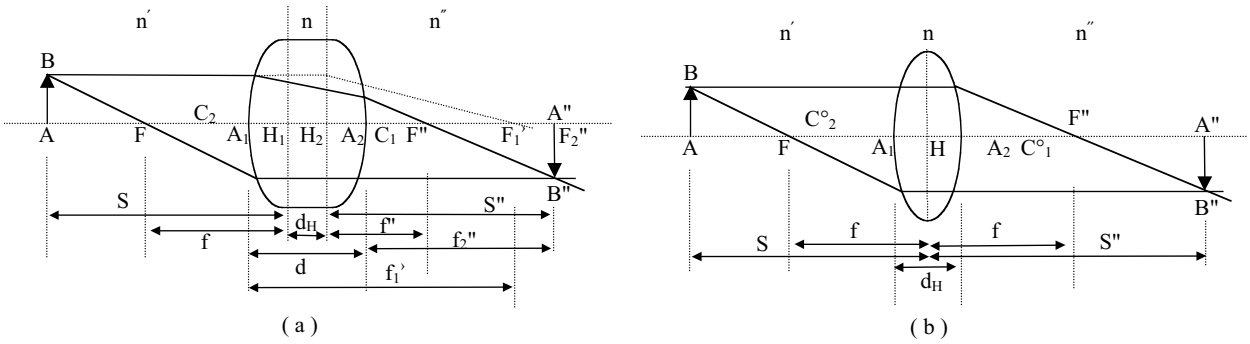

Figure 1. (a) Diagram of the image formed by a thick lens, (b) an equivalent thin lens [12].

In Figure 1 are shown the refractive indices $n^{'}, n, n^{''}$ of the three media separated by two spherical surfaces of centers of curvature C_1 and C_2 or C_1° and C_2° and back focal lengths $f_1^{'}$ and f_2", the latter two of which are measured from the vertices A_1 and A_2 to the corresponding secondary focal points $F_1^{'}$ and F_2". The front and back equivalent focal lengths f and f'' are measured from the focal points F and F'' to the respective principal points H_1 and H_2. In the case of thin lens, H_1 and H_2 are superimposed on H. The object AB is located at distance S, and its real image, $A''B''$, is formed at the distance $S^{'}$, both distances being measured from the principal planes [12].

Let us consider a thick lens as shown in Figure 1(a) where the lens faces have radii of curvature R_1 and R_2. The equivalent thin lens is shown in Figure 1(b). This equivalence can be revealed better with a matrix formalism. With the notations in Figure 1, when $n^{'} = n^{''}$ the matrix of the thick lens is [13, 14]

$$M = \begin{bmatrix} 1 - \frac{d}{f_1^{'}} & \frac{d}{n} \\ \frac{-n}{f_1^{'}} - \frac{1}{f_2^{''}} + \frac{d}{f_1^{'} f_2^{'}} & 1 - \frac{d}{n f_2^{''}} \end{bmatrix}. \tag{1}$$

The distances from vertices A_1 and A_2 to the principal planes H_1 and H_2, respectively, are

$$A_1H_1 = h_1 = \frac{fd}{nf_2^{''}} \tag{2}$$

$$A_2H_2 = -h_2 = \frac{-fd}{f_1^{'}}. \tag{3}$$

With this notation the matrix of the thick lens is

$$M = \begin{bmatrix} 1 - \frac{h_2}{f} & d_e \\ -\frac{1}{f} & 1 - \frac{h_1}{f} \end{bmatrix} \tag{4}$$

and it is equivalent to the following succession:

$$M = \begin{bmatrix} 1 & h_2 \\ 0 & 1 \end{bmatrix} \begin{bmatrix} 1 & 0 \\ -\frac{1}{f} & 1 \end{bmatrix} \begin{bmatrix} 1 & h_1 \\ 0 & 1 \end{bmatrix}. \tag{5}$$

That is, thick lens is equivalent to a thin lens of the same focal length placed between two spaces h_1 and h_2. The effective thickness d_e of the thick lens is

$$d_e = \frac{d}{n} = h_1 + h_2 - \frac{h_1 h_2}{f}. \tag{6}$$

By using thick lens formulas, we obtain for the distance d_H measured between the principles planes H_1 and H_2 the equation

$$d_H = (1- \in) d_e \tag{7}$$

where

$$\in = \frac{R_2 - R_1}{[n(R_2 - R_1) + d(n-1) R_2 R_1]} \tag{8}$$

is an dimensionless parameter that indicates the fractional difference between distances d_e and d_H [13].

Note that the focal length of the thick lens can be given in a form that is similar to that of an infinitesimally thin lens,

$$\frac{1}{f} = (n-1)\left(\frac{1}{R_1^o} - \frac{1}{R_2^o}\right) \tag{9}$$

with

$$R_i^o = (\in n) R_i. \tag{10}$$

A system of two thin lenses of focal lengths f_1 and f_2 placed at a distance d is equivalent to a thick lens:

$$\begin{bmatrix} 1 & 0 \\ -\frac{1}{f_2} & 1 \end{bmatrix} \begin{bmatrix} 1 & d \\ 0 & 1 \end{bmatrix} \begin{bmatrix} 1 & 0 \\ -\frac{1}{f_1} & 1 \end{bmatrix} = \begin{bmatrix} 1 - \frac{d}{f_1} & d \\ \frac{-n}{f_1} - \frac{1}{f_2} + \frac{d}{f_1 f_2} & 1 - \frac{d}{f_2} \end{bmatrix}. \tag{11}$$

Generally a thick lens, which is characterized by the matrix

$$M = \begin{bmatrix} A & B \\ C & D \end{bmatrix}, \tag{12}$$

where A, B, C and D are real and

$$\det M = AD - BC = 1, \tag{13}$$

is equivalent to a thin lens of focal length f placed between two spaces of lengths h_1 and h_2:

$$M = \begin{bmatrix} 1 & \frac{A-1}{C} \\ 0 & 1 \end{bmatrix} \begin{bmatrix} 1 & 0 \\ C & 1 \end{bmatrix} \begin{bmatrix} 1 & \frac{D-1}{C} \\ 0 & 1 \end{bmatrix}, \tag{14}$$

where

$$C = -\frac{1}{f} \tag{15}$$

$$h_1 = \frac{D-1}{C} and \tag{16}$$

$$h_2 = \frac{A-1}{C}. \tag{17}$$

It is also equivalent to a system of two thin lenses of focal lengths f_1 and f_2 placed at a distance d:

$$M = \begin{bmatrix} 1 & 0 \\ \frac{D-1}{B} & 1 \end{bmatrix} \begin{bmatrix} 1 & B \\ 0 & 1 \end{bmatrix} \begin{bmatrix} 1 & 0 \\ \frac{A-1}{B} & 1 \end{bmatrix} \tag{18}$$

where

$$-\frac{1}{f_1} = \frac{A-1}{B} \tag{19}$$

$$-\frac{1}{f_2} = \frac{D-1}{B} \tag{20}$$

and

$$d = B. \tag{21}$$

The general relations are useful in optical computations [14].

2.2. Equivalent Thick and Thin Thermal Lenses

In optically pumped laser rods, due to the temperature gradient, the real part of the refractive index varies quadratically with distances r from the optical axis [15]:

$$n = n_o - \frac{n_2 r^2}{2}. \tag{22}$$

The matrix of a laser rod of length d reads

$$M = \begin{bmatrix} \cos\gamma d & (n_o\gamma)^{-1}\sin\gamma d \\ -n_o\gamma\sin\gamma d & \cos\gamma d \end{bmatrix}, \tag{23}$$

where

$$\gamma^2 = \frac{n_2}{n_o}, \tag{23a}$$

and it depends on the total heat dissipated in the rod volume [16]. Thus, the rod acts as a lens-like medium, that is, as a thick lens of focal length f, effective thickness d_e, and distance h of the principal planes from the rod ends given by

$$\frac{1}{f} = n_o\gamma\sin\gamma d \tag{24}$$

$$d_e = \frac{\sin\gamma d}{n_o\gamma} \tag{25}$$

$$h = \frac{\tan\frac{\gamma d}{2}}{n_o\gamma}. \tag{26}$$

The distance d_H between the principal planes can be Equation (7) written in the form

$$d_H = (1- \in)\, d_e \tag{27}$$

with

$$\in = 1 + \tan^2\frac{\gamma d}{2}. \tag{28}$$

One then obtains

$$2h = \in d_e. \tag{29}$$

From Equation (28) one can see that $\in > 1$, and then $d_H < 0$ and $2h > d_e$.

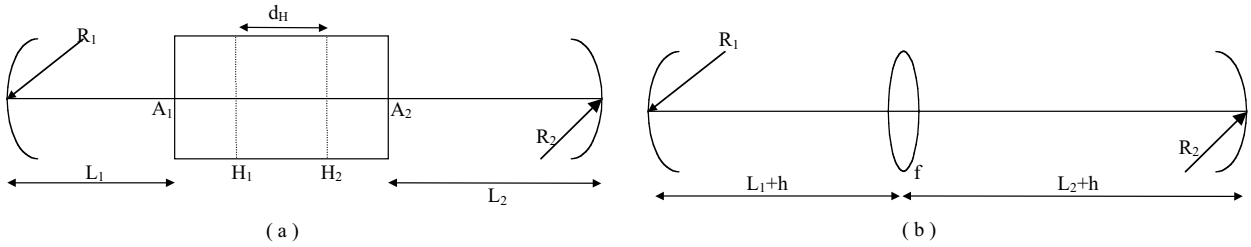

Figure 2. (a) Solid – state laser resonator with a lens-like rod; (b) equivalent resonator with a thin lens [16]

In Figure 2 H_1, H_2 are the primary and secondary principal planes, respectively, placed at distances $A_1H_1 = A_2H_2 = h$ from the rod ends [16].

Therefore, when one takes into account the equivalence relations of thick and thin lenses, a longer equivalent resonator with a thin lens placed in the middle of the rod results, as shown in Figure 2. In many cases, especially when the stability under pump – induced fluctuations is analyzed, because h is dependent on γ, it is correct to consider the distances L_1 and L_2 from the mirrors of the resonator to the ends of the rod, and thus the distances from the mirrors to the thin thermal lens $L_1 + h$ and $L_2 + h$. In Section 2.3 – 2.5 we deal with distances from the resonator mirrors to the rod ends.

2.3. Linear Resonator Containing a Laser Rod with Curved Endfaces

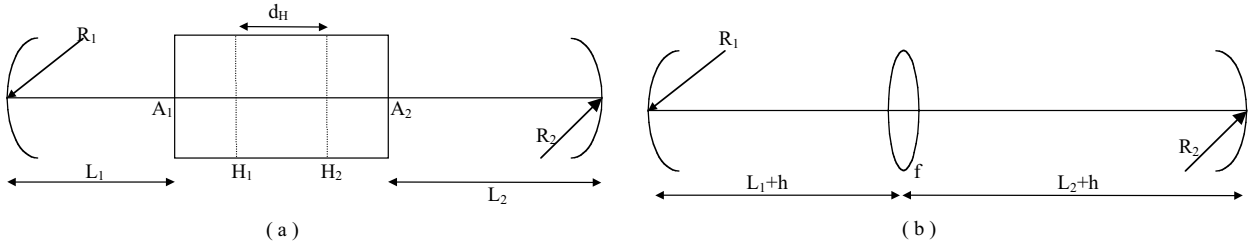

Figure 3. (a) Linear laser cavity containing a rod with curved end faces of radius $R^{'}$; (b) equivalent resonator with the two curved end faces of the laser rod represented by two thin lenses of focal length $f^{'}$ [17, 18].

Let us consider the linear laser cavity schematically shown in Figure 3(a). It is bound by two spherical mirrors of radii R_1 and R_2, and it contains a laser rod of length d with curved end surfaces of radius $R^{'}$. The equivalent resonator is shown in Figure 3(b), where $-1/f' = (n_o - 1)/R'$. By using a matrix formalism [17, 18], one obtains the effective resonator length

$$L^* = \left(L_1^{'} + L_2^{'} - \frac{2L_1^{'}L_2^{'}}{h}\right)\left(1 - \frac{h}{f'}\right) - L_1^{'}L_2^{'}\left(\frac{1}{f} - \frac{2}{h}\right) \tag{30}$$

where

$$L_i^{'} = L_i + h - \frac{hL_i}{f'}; i = 1, 2 \tag{31}$$

The g_i^* parameters of this resonator are

$$g_i^* = 1 - L_j^{'}\left[\frac{1}{f} + \frac{2}{f'} - \frac{h}{ff'}\right] - \frac{L^*}{R_i}. \tag{32}$$

When the rod has plane end faces ($R^{'} = \infty$ and $^1\!/_{f'} = 0$) equations (30) and (32) reduce to the well–known relations for a resonator with a thin lens inside. The matrix M of the resonator that corresponds to a plane E_j at one mirror inside the resonator is

$$M = \begin{pmatrix} A_i & B_i \\ C_i & D_i \end{pmatrix} \tag{33}$$

where

$$A_i = 2g_1^*g_2^* - 1 + \frac{2L^*g_j^*}{R_i} \tag{34}$$

$$B_i = 2g_j^*L^* \tag{35}$$

$$D_i = 2g_1^*g_2^* - 1 - \frac{2L^*g_j^*}{R_i} and \tag{36}$$

$$C_i = \frac{(A_iD_i - 1)}{B_i}. \tag{37}$$

(See Ref. [19]).

The stability condition is well known:

$$0 < g_1^*g_2^* < 1. \tag{37.a}$$

Equation (32) indicates that g_i^* parameters have a linear dependence of $^1\!/_f$. The intersections of the $^1\!/_f$ line with the axes g_i^*= 0, i = 1, 2 and with the hyperbola $g_1^*g_2^* = 1$ give the critical values of $^1\!/_f$ that correspond to edges of the stability regions:

$$\frac{1}{f} = \frac{1}{1 - \frac{h}{f'}}\left[-\frac{2}{f^1} + \frac{1}{h + \delta_1\left(1 - \frac{h}{f'}\right)} + \frac{1}{h + \delta_2\left(1 - \frac{h}{f'}\right)}\right], \tag{38}$$

where δ_1 and δ_2 have the following values:

$$\begin{gathered} \delta_1 = L_2\delta_2 = L_1 - R_1 for g_1^* = 0 \\ \delta_1 = L_1\delta_2 = L_2 - R_2 for g_2^* = 0 \\ \delta_1 = L_1\delta_2 = L_2 for g_1^*g_2^* = 1 \\ \delta_1 = L_1 - R_1\delta_2 = L_2 - R_2 for g_1^*g_2^* = 1 \end{gathered} \quad . \tag{39}$$

When the laser rod has plane endfaces ($R^{'} = \infty$ and $^1\!/_{f'} = 0$), Equations (38) reduces to

$$\frac{1}{f} = \frac{1}{(h + \delta_1)} + \frac{1}{(h + \delta_2)}. \tag{40}$$

The critical values of $^1\!/_{f'}$ corresponding to the edges of the stability regions are obtained from Equation (38):

$$\frac{1}{f'} = \frac{\left(\frac{1}{\delta_1} + \frac{1}{\delta_2}\right)}{2} + \frac{1 - \frac{1}{\left(2 - \frac{h}{f}\right)}}{h} \pm \left\{ \frac{\left(\frac{1}{\delta_1} - \frac{1}{\delta_2}\right)^2}{4} + \frac{1}{\left[h\left(2 - \frac{h}{f}\right)\right]^2} \right\}^{1/2}. \tag{41}$$

The simple elements of the matrix presented are useful for the resonator analysis. Relations for the beam waist and its location have simple forms in terms of g parameters.

2.4. Symmetrical Ring Resonator

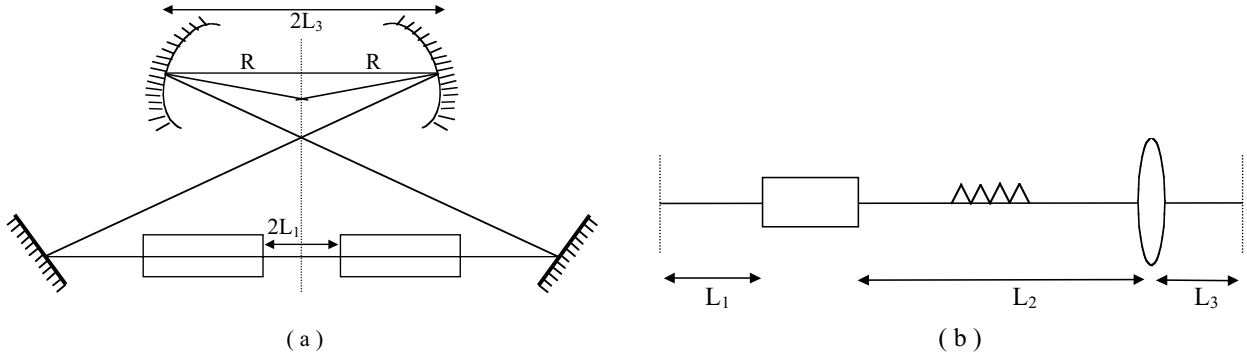

Figure 4. (a) Symmetrical ring cavity including two laser rods; (b) equivalent linear sequence for half of the ring cavity [12].

Let us consider the symmetrical cavity shown in Figure 4(a). It contains two laser rods and two plane and two spherical folding mirrors and is equivalent to twice the linear sequence represented in Figure 4(b). We use the following notations:

$$\frac{1}{f_e} = \frac{2\left(1 - \frac{2L_3}{R}\right)}{R} \tag{42}$$

$$h_e = \frac{h + L_2 + L_3}{\left(1 - \frac{2L_3}{R}\right)} \tag{43}$$

$$g_e = 1 - \frac{h_e}{f} \tag{44}$$

$$L = L_1 + h + h_e \tag{45}$$

$$L' = L - \frac{h_e\left(L_1 + h\right)}{f}. \tag{46}$$

One obtains the effective resonator length for a round trip by starting at the median plane between the spherical mirrors:

$$L^* = 2\left\{ L - \left(L'\right)^2 \left[\frac{1}{f_e} + \frac{1}{f g_e}\right] + \frac{h_e^2}{f g_e} \right\} \tag{47}$$

The effective g^* parameter is

$$g^* = 1 - 2L'\left(\frac{1}{f} + \frac{g_e}{f_e}\right). \tag{48}$$

Then the matrix M of the symmetrical ring resonator corresponding to the plane between the spherical mirrors is

$$M = \begin{bmatrix} 2\left(g^*\right)^2 - 1 & 2g^*L^* \\ 2g^*\frac{\left(g^*\right)^2-1}{L^*} & 2\left(g^*\right)^2 - 1 \end{bmatrix} = \left[\pm \begin{pmatrix} g^* & L^* \\ \frac{\left(g^*\right)^2-1}{L^*} & g^* \end{pmatrix} \right]^2. \tag{49}$$

The resonator is stable for $-1 < g^* < 0$ and $0 < g^* < 1$. The critical values of $1/f$ corresponding to the edges of the stability regions are

$$\frac{1}{f} = \begin{cases} \frac{1}{L_2+h-\frac{R}{2}} for g^* = 1 \\ \frac{1}{h_e} + \frac{1}{L_1+h} \end{cases} \tag{50}$$

$$\frac{1}{f} = \begin{cases} \frac{1}{h_e} for g^* = -1 \\ \frac{1}{L_1+h} + \frac{1}{L_2+h-\frac{R}{2}} \end{cases} \tag{51}$$

$$\frac{2}{f} = \frac{1}{L_1+h} + \frac{2-\frac{1}{1-\frac{h_e}{f_e}}}{h_e} \pm \left\{ \frac{1}{\left(L_1+h\right)^2} + \frac{1}{\left[h_e\left(1-\frac{h_e}{f_e}\right)\right]^2} \right\}^{1/2} for g^* = 0. \tag{52}$$

At given values of f, h, R and L_1 one obtains the following relations for L_2 as a function of L_3 corresponding to the edges of the stability regions :

$$L_2 = \begin{cases} \frac{f-h+R}{2} for g^* = 1 \\ \frac{1}{\frac{1}{f}-\frac{1}{L_1+h}} - h - \frac{L_3}{1-\frac{2L_3}{R}} \end{cases} \tag{53}$$

$$L_2 = \begin{cases} \frac{1}{\frac{1}{f}-\frac{1}{L_1+h}} - h - \frac{R}{2} for g^* = -1 \\ \frac{f-h+L_3}{1-\frac{2L_3}{R}} \end{cases} \tag{54}$$

$$L_2 = f - h + \frac{R}{2} + \frac{f^2}{2\left(L_1+h-f\right)} - \frac{R^2}{4\left(R-2L_3\right)} \pm \frac{\left\{ \frac{f^4}{\left(L_1+h-f\right)^2} + \frac{R^4}{4\left(R-2L_3\right)^2} \right\}^{1/2}}{2} \tag{55}$$

for $g^* = 0$.

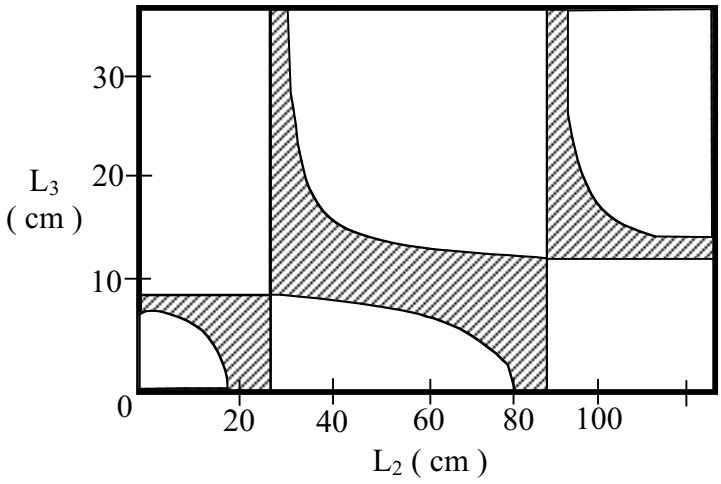

Figure 5. Stability zones illustrated by the hatched area in the (L_2, L_3) plane for the symmetrical ring resonator of Figure 3. with $R = 20$cm, $L_1 = 20$cm, the length of one rod $d = 10$cm, $n_o = 1.85$ and $\gamma = 0.0566$ [17, 18].

A diagram of stability in terms of L_2 and L_3 is shown in Figure 4. The two vertical lines and four curves that delimit the stability regions are given by Equations (53), (54) and (55).

For a confocal symmetrical ring resonator, when $R = 2L_3$, the matrix M corresponding to the median plane between the spherical mirrors is;

$$M = \begin{bmatrix} g^* & L^* \\ \frac{(g^*)^2-1}{L^*} & g^* \end{bmatrix}, \tag{56}$$

where

$$g^* = -1 + \frac{2L^{'}}{f} \tag{57}$$

$$L^* = 2L^{'}\left[\frac{L_1+h}{f} - 1\right] \tag{58}$$

$$L^{'} = L_1 + L_2 + 2h - L_3 - \frac{(L_1+h)(L_2+h-L_3)}{f}. \tag{59}$$

The critical values of $^1/_f$ corresponding to the edges of the stability regions are

$$\frac{1}{f} = \begin{cases} \frac{1}{L_1+h} for g^* = 1 \\ \\ \frac{1}{L_2+h-L_3} \end{cases} \tag{60}$$

$$\frac{1}{f} = \begin{cases} 0 for g^* = -1 \\ \\ \frac{1}{L_1+h} + \frac{1}{L_2+h-L_3} \end{cases} \tag{61}$$

$$\frac{1}{f} = \frac{1}{L_1+h} + \frac{1}{L_2+h-L_3} \pm \left\{ \frac{1}{(L_1+h)^2} + \frac{1}{(L_2+h-L_3)^2} \right\}^{1/2} for g^* = 0. \tag{62}$$

2.5. Asymmetric Ring Resonator

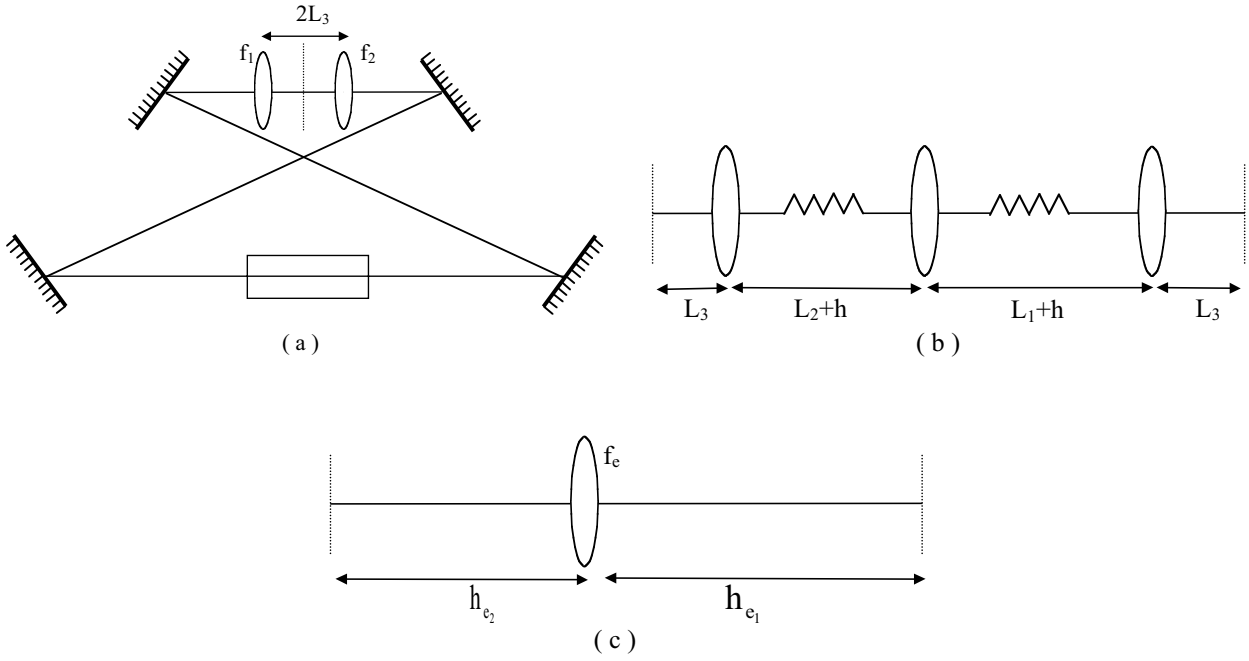

Figure 6. (a) Schematic of a typical asymmetric ring resonator; (b) the equivalent linear sequence for a clockwise round trip starting at the median plane between the focusing elements; (c) simple system of a thin lens placed between two spaces, which is equivalent to the clockwise round trip [12].

Let us consider the asymmetric ring cavity shown in Figure 6(a). It contains one laser rod, two focusing elements such as spherical mirrors or lenses and a convenient number of plane mirrors to complete the ring. The linear sequence, which is equivalent to a clockwise round trip that starts at the median plane between the focusing elements, is shown in Figure 6(b). Finally, it is equivalent to a thin lens placed between two spaces as shown in Figure 6(c). The corresponding matrix is:

$$M = \begin{bmatrix} g_1^* & L^* \\ \frac{g_1^* g_2^* - 1}{L^*} & g_2^* \end{bmatrix}, \tag{63}$$

where

$$g_i^* = 1 - \frac{h_{e_i}}{f_e} \tag{64}$$

$$L^* = h_{e_1} + h_{e_2} - \frac{h_{e_1} h_{e_2}}{f_e} \tag{65}$$

with the following notation:

$$L^{'} = L_1 + L_2 + 2h - \frac{(L_1 + h)(L_2 + h)}{f} \tag{66}$$

$$\frac{1}{f_e} = \frac{1}{f} + \frac{1}{f_1} + \frac{1}{f_2} - \frac{L^{'}}{f_1 f_2} - \frac{\left[\frac{(L_1+h)}{f_1} + \frac{(L_2+h)}{f_2}\right]}{f} \tag{67}$$

$$\frac{h_{e_i}}{f_e} = \frac{L_3}{f_e} + \frac{L^{'}}{f_j} + \frac{(L_i + h)}{f} \tag{68}$$

The stability condition is

$$-1 < \frac{g_1^* + g_2^*}{2} < +1 \tag{69}$$

$$g_1^* g_2^* 1/\mathrm{f} \tag{70}$$

(See Ref. [22]).

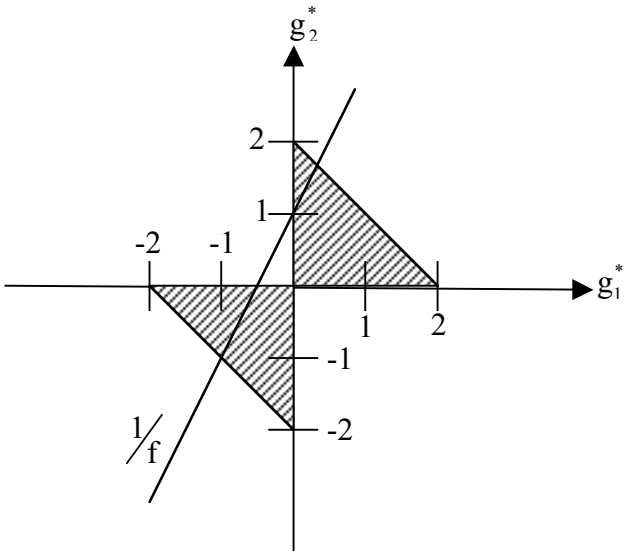

Figure 7. Stability zones illustrated by the hatched area for the asymmetric ring resonator of Figure 6. The point (g_1^*, g_2^*) representing the resonator moves linearly with the dioptric power $1/f$ of the thermal lens along the straight line [22].

A simple diagram of stability is shown in Figure 7. The intersections of the $1/f$ line with the axes $g_i^* = 0$, i = 1,2 and with the $g_1^* + g_2^* = \pm 2$ lines give the critical values of $1/f$ corresponding to the edges of the stability regions:

$$\frac{1}{f} = \frac{\left(1 - \frac{L_3}{f_i}\right)}{L_{e_i}} + \frac{1}{(L_j + h - f_j)} for g_i^* = 0; \tag{71}$$

$$\frac{1}{f} = \frac{-\left[\pm 2 - 2 + (L_1 - L_2)\left(\frac{1}{f_1} - \frac{1}{f_2}\right) + 2\left(\frac{L_{e_1}}{f_2} + \frac{L_{e_2}}{f_1}\right)\right]}{\left[L_{e_1}\left[1 - \frac{(L_2+h)}{f_2}\right] + L_{e_2}\left[1 - \frac{(L_1+h)}{f_1}\right]\right]} for g_1^* + g_2^* = \pm 2, \tag{72}$$

where

$$L_{e_i} = L_i + L_3 + h - \frac{L_3\,(L_i + h)}{f_i}. \tag{73}$$

3. Results and Conclusion

The simple elements of a matrix can be used for an extended analysis of this resonator. In this study simple relations are investigated for the resonators of Nd:Glass and Nd:YAG lasers. Nd:Glass and Nd : YAG lasers simple relations of thick and thin lenses have been applied. Finally, the stability condition is well known: $0 < g_1^* g_2^* < 1$.

References

[1] O. Svelto, Principles of Lasers, Hanna, D.C., 18 (1982).

[2] T.J. Verdeyen, Laser Electronics, New York, 15 (1981).

[3] A. Yariv, Introduction to Optical Electronics, Holt, Reinhart Winston, New York Chap. 5, 479 (1985).

[4] D. Findlay and D.W. Goodwin, The Nd : YAG Laser, in Advances in Quantum Electronics, Vol. 1, 77 - 128, New York (1970).

[5] J.G. Danielmeyer, Progress in Nd : YAG Lasers, in Lasers, New York, Vol. 4, Chap. 1, (1976).

[6] E. Snitzer and C.G. Young, Glass Lasers, in Lasers, New York, Vol. 2, Chap. 1 (1968).

[7] W. Koecher, Solid - State Lasers Engineering, Springer - Verlag, New York, Chap. 7, (1976)

[8] D. Metcalf, P. de Giovanni, J. Zacharowski and M. Leduc, Laser resonators containing self - focusing elements, App. Opt. 26, 4508 - 4517 (1987).

[9] H. Kogelnik and T. Li, Lasers and resonators, App. Opt. 5, 1550 - 1567 (1966).

[10] CRC, Handbook of Lasers with Selected Data on Optical Technology, USA, Section 4, 421 - 441 (1971).

[11] H.P. Kortz, R. Ifflander, and et. al., Stability and Beam divergence of multimode lasers with internal variables lenses, App. Opt. 20, 4124 - 4134 (1981).

[12] V. Magni, Resonators for solid - state lasers with large - volume fundamental mode and high alignment stability, App. Opt. 25, 107 - 117 (1986).

[13] J.S. Uppal, J.C. Monga and et. al., Analysis of an unstable confocal ring laser with a thermally induced active medium, App. Opt. 25, 1389 - 1393 (1986).

[14] F.A. Jenkins and H.E. White, Fundamentals of Optics, Mc.Graw - Hill, New York, Chap. 5, pp. 62 - 81 (1957).

[15] A.E. Siegmann, Lasers, University Science, Hill Valley, California, Chap. 15 (1986).

[16] M. Born and E. Wolf, Principles of Optics, 6^{th} ed., Pergamon, Oxford, Sec. 6.6 (1980).

[17] W.H. Steier, Unstable Resonators, in Laser Handbook, ed. by M.L. Stitch, North - Holland, Amsterdam, Vol. 3, pp. 3 - 39 (1979).

[18] D.B. Rensch and A.N. Chester, Laser Resonators, App. Opt. 12, 997 (1982).

[19] R.H. Pantell and H.E. Puthoff, Fundamentals of Quantum Electronics, Wiley, New York, Chap. 6, Sec. 6 (1969).